International Journal of Progressive Sciences and Technologies (IJPSAT)
ISSN: 2509-0119.

http://ijpsat.ijsht-journals.org
Vol. 22 No. 1 August 2020, pp. 67-81

DFT Study on Electronic Charge Distribution and Quantum−Chemical Descriptors for the Kinetic Stability of Vanadium Aquo Complex Ions $[V(H_2O)_6]^{2+}$ and $[V(H_2O)_6]^{3+}$

Anant Babu Marahatta[1, 2]

[1]Department of Chemistry, Amrit Science Campus, Tribhuvan University, Kathmandu, Nepal

[2]Chemistry Subject Committee, Kathford International College of Engineering and Management (Affiliated to Tribhuvan University), Kathmandu, Nepal

Abstract – Despite the predominant existence of $[V(H_2O)_6]^{2+}$ and $[V(H_2O)_6]^{3+}$ complex ions in medicinal and biological fluid matrices, their critical roles in electrochemical, environmental, and industrial aspects of chemistry, and their typical chemical properties including high chemical instability, and fast disproportionation type chemical reactions, an in−depth study concentrated on electronic charge distributions in them and their relative chemical reactivity through quantum mechanical molecular orbitals approach is rarely available. In this insight, the hybrid density functional B3LYP with 6−31G (*d*, *p*) basis set has been employed computationally, and calculated Mulliken atomic charges distribution, HOMO−LUMO interactions and their band gaps (ΔE_{gap}), and global quantum−chemical descriptors (QCDs) for these two aquo complex ions separately. The general results depict that the $[V(H_2O)_6]^{2+}$ ion has a: (1) higher oxidation tendency (*IP* = 11.332 eV), (2) stronger electron donating propensity (*EA* = 8.377 eV), (3) lower polarizability, (η = 1.477 eV, σ = 0.677 eV), and (4) weaker electrophilic character (ω = 32.871 eV) than the $[V(H_2O)_6]^{3+}$ ion (*IP* = 18.445 eV, *EA* = 15.772 eV, η = 1.336 eV, σ = 0.748 eV, and ω = 109.537 eV). Moreover, the theoretically predicted wavelengths λ_1 = 420.17 nm (violet), and λ_2 = 494.81 nm (green) of the visible light to be absorbed respectively by $[V(H_2O)_6]^{2+}$ and $[V(H_2O)_6]^{3+}$ complex ions in their aqueous solutions have confirmed their real practical colors. The major significance and novelty of this study lies in elucidating relative kinetic stability of the V (II) and V (III) aquo complex ions through *ab initio* type quantum mechanical method.

Keywords – V^{2+}/V^{3+} hydrated complexes, Mulliken charges, HOMO−LUMO interactions and energy gaps, and Global chemical reactivity descriptors.

I. INTRODUCTION

As vanadium metal of the 3*d* series in periodic table is typically featured by its incomplete *d*-orbital, high propensity for forming distinctive colored complexes, intense hydration reactions, variable oxidation states etc., its complex compounds featuring vanadium−ligand coordinate bonds ($L \rightarrow V^{n+}$) and the V^{n+} coordination centers are of both scholarly and practical interests [1], [2], [3]. Being the coordination chemistry of same type but homoleptic vanadium aquo complexes with $H_2O \rightarrow V^{n+}$ only bonds more prominent in electrochemical, environmental, catalytic, industrial, biological, and medicinal aspects of chemistry due to the accessibility of its four adjacent oxidation states (V^{n+}; n = +II, +III, +IV, and +V) for producing characteristic colored aquo complexes: $[V(H_2O)_6]^{2+}$ (lilac), $[V(H_2O)_6]^{3+}$ (green), $[VO(H_2O)_5]^{2+}$ (blue), and $[VO_2(H_2O)_3]^{+}.H_2O$ (yellow) respectively in the aqueous type media (both in the medicinal and biological fluid matrices) [4], [5], the detailed investigations of electronic distribution in them and their molecular orbitals (hereafter, MOs) interactions plus global chemical reactivity descriptors are more crucial not only for modeling the vanadium hydrolysis reactions in the aqueous type media but also for understanding their partial atomic charges distribution and reaction kinetics (chemical reactivity and stability) quantitatively. In theoretical/computational chemistry, many important physical observables such as

Corresponding Author: Anant Babu Marahatta

energies of the MOs and their electronic configurations, highly populated energy levels (frontier sites of electron occupation i.e. frontier molecular orbitals, hereafter, FMOs: highest occupied molecular orbital (hereafter, HOMO), and lowest unoccupied molecular orbital (hereafter, LUMO)) and their eigenvalues, partial atomic charges distribution, electric dipole moments etc. can be derived through the MOs approach of quantum chemistry from which one can describe and measure the relative intensity of chemical reactivity or stability of any molecular specimens quantitatively. In such complex computational quantum mechanical approach, a repeated mathematical process is involved which on the fly computes wave function and energy at a starting (trial) molecular geometry, tests various possibilities to see which atomic arrangements and the electrons around them give the lowest energy value, determines the magnitudes of almost all aforementioned physical observables quantitatively, and then proceeds towards yielding a low energy ground state electronic structure [6]. Among the wide varieties of theoretical models offered by the *Gaussian:* an electronic structure package, the density functional theory (hereafter, DFT) model is most popularly known for its extraordinary ability to implement such complicated type quantum mechanical procedures in the limited computational resources [7], [8]. This spatially dependent electron density based quantum mechanical model is mostly used in chemistry, physics, and material science for exploring ground state electronic structures of the multi−electron atomic or molecular systems, calculating FMOs and their eigenvalues, determining global chemical reactivity descriptors, and Mulliken atomic charges distribution theoretically [8], [9], [10], [11], [12], [13]. In spite of the DFT's approximate formalism for solving Schrodinger's wave equation iteratively [14], the increasingly successful trend of it is mainly due to the fact that it attributes very reliable quantum chemical computations by associating molecule's ground-state electron density significantly (Hohenberg−Kohn theorem), and gives better results than *ab initio* electronic structure methods at the similar computational cost [7], [8], [15]. More importantly, the performance of this model while applying to coordination and transition metal based complex compounds is awesome as reported in previously published research and review papers [16], [17], [18], [19], [20], [21]. In these scientific reports, almost all the authors have highlighted the utmost potentiality of the DFT model, and underscored its skills to offer quite impressive explanation for elucidating experimentally observed molecular physicochemical properties of the 3*d* transition metal compounds.

Being the vanadium a ubiquitously present element in the Earth's crust, and hydrospheric and atmospheric regions, its catalytic and medicinal properties, and highly useful low molecular weight coordination complexes are widely recognized [22], [23], [24]. For example, in the oceanic algae, vanadium is used as an active enzymatic center; in some marine invertebrates (subphylum *Tunicata*), the vanadium complexes with +III, +IV or +V oxidation states serve as a defense mechanism [24]; in the wide varieties of human foods (such as mushrooms, spinach, dairy products, vegetable oils, whole grains and cereals etc.), vanadium is present as a trace mineral which can manage diabetes etc. Additionally, varieties of vanadium and its compounds based therapeutic drugs are already proposed to treat many deadliest and parasitic human diseases [25], [26], and even sometime the vanadium supplements are given to people suffering from vanadium deficiency as a dietary micronutrient. Despite being such extremely necessary bioelement, and precursor element of several vanadium based compounds that can demonstrate significant catalytic, and medicinal properties if and only if they remain suspended in the aqueous matrices, the research works related to reveal atomic charge distribution and global quantum−chemical reactivity parameters such as HOMO−LUMO interactions and their energy gap (ΔE), ionization potential (IP), electron affinity (EA), chemical hardness (η), chemical softness (σ), electronic chemical potentials (μ), electrophilicity index (ω), and electronegativity (χ) of their predominant aquo complexes in oxidation states +II, +III, +IV, and +V : $[V(H_2O)_6]^{2+}$, $[V(H_2O)_6]^{3+}$, $[VO(H_2O)_5]^{2+}$, and $[VO_2(H_2O)_3]^{+}.H_2O$ are very limited. However, this study is mainly concentrated in the first two aquo complexes because of considering their relatively more chemical instabilities, self−exchange electron transfer reactions, high oxidation−reduction tendencies, and fast disproportionation type chemical reactions. As they are most frequently encountered while carrying out several industrial aqueous type chemical reactions in a number of potential applications: V_2O_5 is used as a catalyst for manufacturing sulfuric acid through contact process; $[V(H_2O)_6]^{2+}/[V(H_2O)_6]^{3+}$ redox couple is used as anolyte solution in vanadium redox flow battery (VRFB) system etc. [4], [5], a thorough study on the significance of those global chemical reactivity descriptors is quite indispensable for understanding their relative chemical stability or reactivity kinetically. Apart from this, computing Mulliken atomic charges in $[V(H_2O)_6]^{2+}$ and $[V(H_2O)_6]^{3+}$ complex ions is very essential to understand the electronic charge distribution in them, and to estimate their partial atomic charges qualitatively; and determining exact value of

each and every reactivity descriptor is also very invaluable to achieve inestimable measures for explaining their chemical stabilities quantitatively. Unlike in experimental researches where very advanced and sophisticated tools are necessary to compute them, in theoretical research, they can be determined comparatively easily but with high precision: the former parameter can be determined through a computationally cheap yet decent Mulliken population analysis method [27]; and the latter reactivity parameters can be calculated quantitatively by computing FMOs of each ionic specimen quantum−mechanically, and working out on the HOMO−LUMO interactions and their energy gaps (ΔE_{gap}) [28], [29]. With this, the present study is mainly aimed at elucidating Mulliken atomic charges distribution and global quantum−chemical reactivity parameters for each of these two vanadium aquo complexes in oxidation states +II and +III theoretically by employing the DFT scheme as a robust computational model. The structure of this paper is organized as follows: the computational details are outlined in section 2, the results and discussions are presented in section 3, and the conclusions are given in section 4.

II. Computational Details

Prior to determine the Mulliken atomic charges distribution and global chemical reactivity parameters for each vanadium aquo complex ion: $[V(H_2O)_6]^{2+}$ and $[V(H_2O)_6]^{3+}$, the most stable electronic structure of them were computed theoretically by using computationally designed molecular models as their trial structures. They were carefully built in *GaussView*: the Gaussian graphical interface [30], and the respective Cartesian coordinates of the atoms were extracted for geometry optimization. The concerned *Gaussian* keywords and methodologies were selected as instructed in *Gaussian 09* manual [31]. The hybrid functional based DFT method known as B3LYP was employed with the basis set of this type: 6−31G (*d*, *p*) i.e. the methodology applied was DFT: B3LYP/6−31G (*d*, *p*). The better and more reliable computational results were assured by using the greater basis set of the type 6−31G (*d*, *p*), where "6−31G" is the standard, split-valence double-zeta basis set: the functions that were used in *Gaussian* script computationally while describing the core and valence orbitals of the atoms; and the functions in parentheses "(*d*, *p*)" are polarization functions on heavy atoms and hydrogen that was used to properly describe chemical bonds. Again, to direct *Gaussian* for running desirable computations, the ionic charge and spin multiplicity were specified as two integers accordingly. Here, both complex ions are cationic with dissimilar positive charge units, *i.e.* $[V(H_2O)_6]^{2+}$ and $[V(H_2O)_6]^{3+}$ have charge units = +2 and +3 respectively. Thus, the respective sets of integers (charge, spin multiplicity) used in the *Gaussian* input file to describe these cationic complexes were (2, 2) and (3, 1) respectively. Moreover, while solving the electronic Schrodinger equation iteratively, the self-consistent field (hereafter, SCF) with both default SCF procedure (SCF=Tight) and Berny algorithm for geometry optimizations to a local minimum were selected in *Gaussian* 09 [31], [32]. In this contribution, only the theoretical results about the electronic charge distribution schemes, and the global quantum−chemical reactivity indicators for $[V(H_2O)_6]^{2+}$ and $[V(H_2O)_6]^{3+}$ complex ions are reported. For this, the *Gaussian* output files of each complex ion (such as *.log*, and *.fchk*) containing three dimensionally displayed chemical data were read by using *GaussView*, and extracted Mulliken atomic charges distribution, MOs and FMOs (HOMO, and LUMO) surface plots, molecular electronic configurations, and the concerned eigenvalues along with visualizing DFT derived ground state electronic structure in the 3D space. While explaining the detailed electronic charge distribution in each complex ion, the respective Mulliken atomic charges were displayed on the DFT derived ground state molecular structure with differently colored spheroids (atoms) by charge distribution; and while determining the values of the following global quantum−chemical reactivity descriptors: ionization potential (*IP*), electron affinity (*EA*), chemical hardness (η), chemical softness (σ), electronic chemical potentials (μ), electrophilicity index (ω), and electronegativity (χ), the HOMO−LUMO energy gap (ΔE_{gap}) was calculated manually on the basis of which all these reactivity parameters were determined quantitatively by using previously formulated mathematical equations Eq. (1−7) described in section 3.2.

III. Results and Discussions

3.1. Mulliken population analysis

A Mulliken population analysis [27] is one of the widely accepted methods used most frequently in the theoretical research which is very often recognized as a powerful computational mean for predicting the values of relative atomic charges of the molecular specimens using localized basis sets. While the computational calculations are on the fly, this method starts to compute Mulliken atomic charges by utilizing the pre−calculated quantum mechanical information obtained from the molecular geometry optimization process. Due to this post−processing type calculation, it is more popularly known among the researchers for its computationally cheapest but fastest skills

to analyze the Mulliken population qualitatively [9]. Even though, it is considered as a less reliable computational mean to produce exact magnitudes of atomic charges in a physically meaningful scale (atomic charges are less absolutely defined), its wide recognitions more especially in examining the electron charge redistribution and bond populations in the bulk materials as well as in simple molecular specimens make itself an indispensable tool in the field of quantum chemistry and physics [33]. Computationally, it can be routinely carried out by those theoretical methods that are based on the LCAO MO (Linear combination of the atomic orbitals molecular orbitals) approximations [31]. As the DFT model is based on LCAO−Kohn−Sham ansatz [7], it can effectively perform Mulliken population analysis by using the selective data sets obtained from its energy minimization process [9], [31]. In this study, the DFT model has been employed computationally and computed Mulliken charges distribution in the vanadium, hydrogen, and oxygen atoms of the vanadium aquo complexes in oxidation states +II and +III. The concerned results derived from it are presented below.

3.1.1 Mulliken atomic charges distribution in $[V(H_2O)_6]^{2+}$ and $[V(H_2O)_6]^{3+}$

The DFT derived Mulliken atomic charges distribution in the vanadium, hydrogen, and oxygen atoms of the V^{2+} and V^{3+} aquo complexes: $[V(H_2O)_6]^{2+}$ and $[V(H_2O)_6]^{3+}$ are presented in Table 1, and Table 2 respectively where all the numerically labeled atoms are listed in accordance with the atomic label of Figure 1(a), and Figure1(b). On the basis of an intensity of Mulliken atomic charges, all the nineteen atoms of the $[V(H_2O)_6]^{2+}$ and $[V(H_2O)_6]^{3+}$ complex ions are colored and displayed as their DFT derived ground state electronic structures (Figure 1), where color indices and range are clearly mentioned. From the color indices of both complex ions, it can be concluded that all the red colored (O2, O4, O6, O8, O10 and O12), the most green colored (V1), and the dark green colored (H3, H5, H7, H9, H11, H13, H14, H15, H16, H17, H18, and H19) spheroids represent the most negatively, most positively, and less positively charged atoms respectively. The same observation can be reconfirmed by analyzing the concerned numeral Mulliken atomic charges listed in Table 1 and Table 2. Such inhomogeneous charge distributions in either of these two complexes are mostly arose due to a strong ability of O atom of each H_2O ligand to attract a bond pair towards itself as its electronegativity (□□in Pauling scale) (□O = 3.44) is significantly greater than that of the V (□V = 1.63) and H (□H = 2.20) atoms. This effect is more pronounced in the vanadium−bonded oxygen atoms which bear maximum partial negative charges: Mulliken charge unit per O atom in (a) $[V(H_2O)_6]^{2+}$: −0.66 *a.u.*, 1.37 times, and in (b) $[V(H_2O)_6]^{3+}$: −0.67 *a.u.*, 1.92 times more in electron density than in the centrally located respective V atoms. This is the reason why central vanadium atoms of them behave as the most "active−sites" (electron deficient) while involving in oxidation and reduction type chemical reactions (any dissolved oxygen in the aqueous solution of V (II) containing $[V(H_2O)_6]^{2+}$ complex ions oxidizes latter into $[V(H_2O)_6]^{3+}$cations, and the aqueous solution of V(III) containing $[V(H_2O)_6]^{3+}$complex ions shows reduction reaction on the surface of metals such as Zn and other metallic sites of electron transfer). Hence, the $[V(H_2O)_6]^{2+}$ and $[V(H_2O)_6]^{3+}$ complex ions behave as powerful reducing and oxidizing agents, and become very unstable in the presence of air and electron transfer metallic sites respectively. Such dissimilar charge distributions in them further make themselves to take part in electron exchange type reactions to each other: $[V(H_2O)_6]^{2+}$ + $[V(H_2O)_6]^{3+} \rightleftharpoons [V(H_2O)_6]^{3+} + [V(H_2O)_6]^{2+}$, and in acid−base reactions: $[V(H_2O)_6]^{z+} \rightleftharpoons [V(H_2O)_5(OH)]^{(z-1)+} + H^+$. The underlying explanation for the first reaction is quite simple as it is processed by the single electron self−exchange mechanism caused by the presence of an unequal atomic charge units in the two central V atoms, whereas the second reaction is governed by the overall charge distributions in the complexes. As the central V atoms of both complex ions are found to be highly positively charged, the bond pair electrons of $V-OH_2$ are pulled away from the O of H_2O towards V, making the electron pairs in the O−H bonds to be pulled towards the O leaving sufficiently positive charge on the H atoms that in turn make themselves to be pulled off as H^+ (Arrhenius acid) in the aqueous solution (Arrhenius base). More specifically, the Mulliken charge units of the V atoms in $[V(H_2O)_6]^{2+}$ and $[V(H_2O)_6]^{3+}$ complexes are calculated as +0.703 *a.u.*, and +1.241 *a.u.* respectively, suggesting that the latter complex ion can exchange its H_2O ligands more slowly with the bulk water (here, it is isotopically labeled as H_2O* for simplicity) than the former ion ($[V(H_2O)_6]^{2+} + H_2O^* \rightarrow [V(H_2O)_5(H_2O^*)]^{2+} + H_2O$). It is because "higher the charge units of the metal coordination centers (here, central V atoms), stronger are the metal−ligand (here, ligands = H_2O) bonds" and hence, slower is the ligand (H_2O) exchange reactions [1].

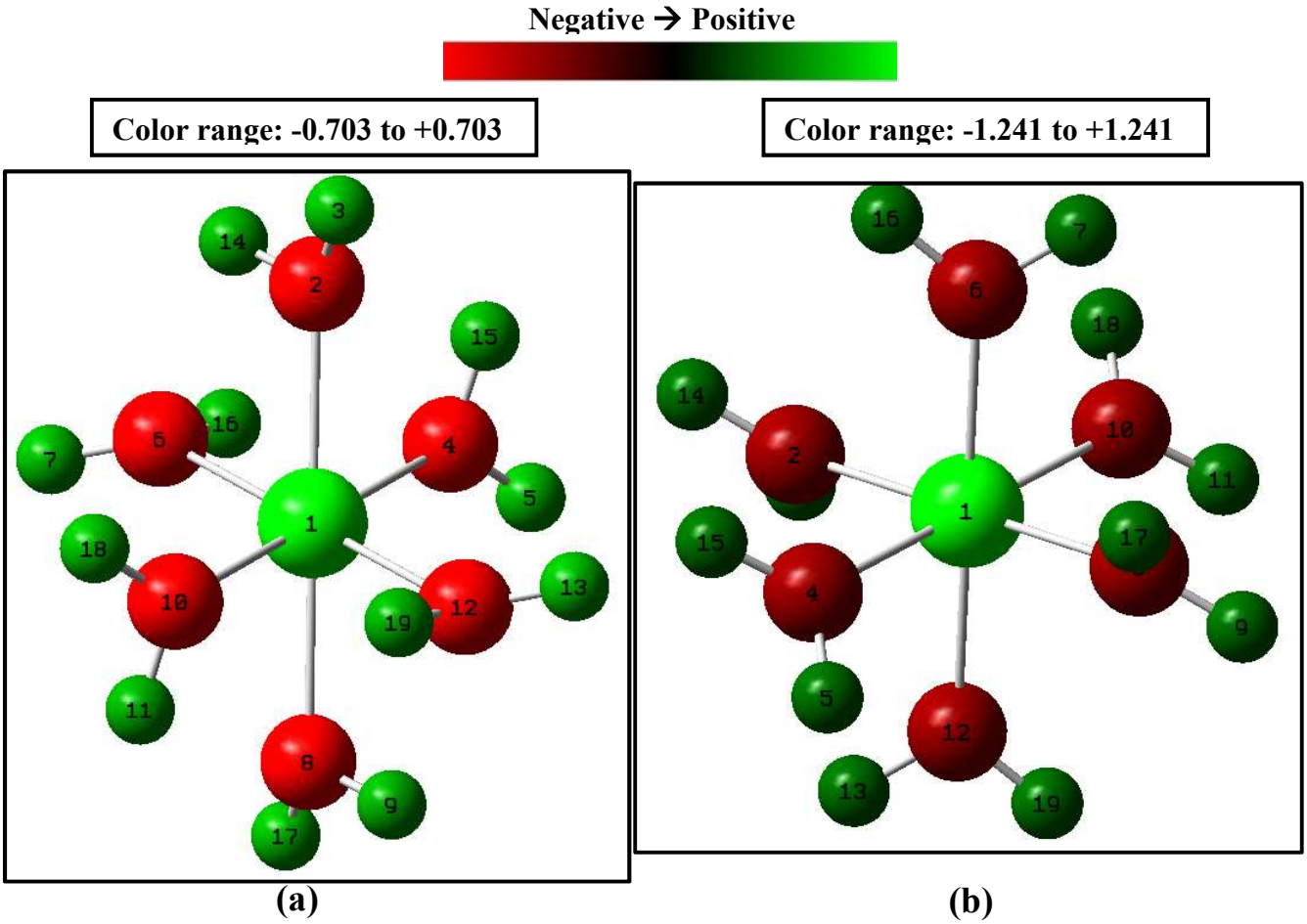

Figure 1. Mulliken charges distribution in the DFT optimized structure of the (a) $[V(H_2O)_6]^{2+}$, and (b) $[V(H_2O)_6]^{3+}$ complex ions. All the atoms are labeled numerically and colored by charge.

Table 1. Mulliken charges (*a.u.*) distribution in the $[V(H_2O)_6]^{2+}$ complex ion.*

Atom label	Charge	Atom label	Charge	Atom label	Charge	Atom label	Charge
V1	+0.703	O6	−0.665	H11	+0.427	H16	+0.424
O2	−0.669	H7	+0.451	O12	−0.665	H17	+0.454
H3	+0.454	O8	−0.669	H13	+0.451	H18	+0.451
O4	−0.654	H9	+0.428	H14	+0.428	H19	+0.424
H5	+0.451	O10	−0.654	H15	+0.427	Sum of Mulliken atomic charges = 2.00 a.u.	

*atom labels are in accordance with Mulliken charges distribution shown in Figure 1(a).

Table 2. Mulliken charges (a. u.) distribution in the [V(H2O)6]3+ complex ion*.

Atom label	**Charge**	**Atom label**	**Charge**	**Atom label**	**Charge**	**Atom label**	**Charge**
V1	+1.241	O6	−0.676	H11	+0.486	H16	+0.486
O2	−0.676	H7	+0.468	O12	−0.676	H17	+0.483
H3	+0.483	O8	−0.676	H13	+0.483	H18	+0.483

O4	−0.676	H9	+0.487	H14	+0.487	H19	+0.486
H5	+0.483	O10	−0.675	H15	+0.486	Sum of Mulliken atomic charges = 3.00 *a. u.*	

*atom labels are in accordance with Mulliken charges distribution shown in Figure 1(b).

Even though, the absolute magnitude of the atomic charges computed by the Mulliken populations analysis displays a high degree of sensitivity to the types of basis set used, the qualitative values of them (for V, H, and O) produced by the DFT:B3LYP/6−31G (*d, p*) method were presented above. In future studies, the total population of each atomic orbital and the gross atomic population plus natural bond order (NBO) analysis will be performed for more accurate determination of the partial atomic charges.

3.2. Molecular orbitals and Global quantum−chemical descriptors

In general, several chemical terminologies, and fundamental electronic concepts of bonding involved in numerous chemical reactions (acid−base, redox, electrophilic, nucleophilic, electron pair donor−acceptor reactions etc.) and in their reaction pathways are to some extent connected to the scale of electron density or electric charge of the molecules and its distribution in them [28]. As explained in section 3.1, the electron charge redistribution and its mode in the ground state electronic structure of the molecules is used to account for their dynamic and static behaviors. Therefore, almost all physicists/chemists/material scientists have been utilizing this generic concept of the electronic theory mostly for understanding various realistic physicochemical phenomena such as locating electron deficient/excess centers, identifying electrophilic/ nucleophilic attacking sites, interpreting proper molecular orientation of the substrates etc. qualitatively. However, on the basis of quantum mechanical theory, the electrons do reside in several types of MOs among which the electronic distribution in the highest energy MO always plays vital role in determining chemical reactivity or stability as quoted by the Nobel Laurette K. Fukui in his historic journal article [34]. As the electrons distribute all over the molecules, their MOs would be comparatively more complicated for large and complex molecular specimens. This is why, the chemists always show their keen interests to those MOs that are most spatially delocalized at the frontier (outer edges) part of the molecules: HOMO and LUMO. The former type MO is known for its low energy, high electron occupancy whereas the latter type is for high energy, zero occupancy (vacant) in the condition of ground state. According to frontier molecular orbital theory, the HOMO and LUMO orbitals and their interactions play significant roles in determining chemical stability of any molecular specimens, and their subsequent analysis provides primary information for explaining intramolecular HOMO−LUMO charge transfer phenomena. Additionally, incorporating HOMO−LUMO orbital interactions with their energy gap (ΔE_{gap}) may provide quantitative explanation for understanding the chemical reactivity or stability of any types of the molecular compounds. In fact, "smaller the HOMO−LUMO energy gap, more is the chemical reactivity of the molecules" i.e. such type molecules show strong ability to donate an electron or an electron pair in the chemical reactions most frequently from the HOMO to the LUMO, further stressing that a proper estimation of the ΔE_{gap} (band gap) for the concerned molecular specimen would be a key to unlock most important physical meanings of some predominant global quantum−chemical reactivity indicators such as: (1) Ionization potential (IP), (2) Electron affinity (EA), (3) Chemical hardness (η), (4) Chemical softness (σ), (5) Electronic chemical potentials (μ), (6) Electrophilicity index (ω), and (7) Electronegativity (χ) [35], [36]. More particularly, such descriptors which are mostly involved to drive the molecular chemical properties are the most prevailing chemical parameters associated with the global chemical reactivity of the transition metal complexes [37], [38], [39].

As the hard and soft acids and bases (hereafter, HSAB) principle is one of the most extensively used concepts for explaining chemical stability of transition metal complexes and their reactions' mechanisms qualitatively [35], it's wide applicability in coordination chemistry mostly for ordering the ligands and transition metal ions relatively with respect to their chemical hardness and softness [36] has made it more fascinating theory. Despite its suitability to those chemical contexts where qualitative descriptions are required, it's quite established mathematical− formulation with the FMO analysis involving HOMO−LUMO interactions and their energy gap ($\Delta E = E_{LUMO} - E_{HOMO}$) gives us an exceptional quantitative explanation while examining molecular reactivity or stability kinetically. In other words, the HSAB theory has been extended to the quantitative aspects of the

ionization potential (*IP*), electron affinity (*EA*), chemical hardness (η), chemical softness (σ), electronic chemical potentials (μ), electrophilicity index (ω), and electronegativity (χ) [37] mathematically. The detailed mathematical derivations and the concerned formulations can be found at any general quantum chemistry text books. The very general expressions based on the mathematical definition of η (η is directly proportional to second order derivative of total energy E (DFT derived) of a chemical system with respect to changes in the number of electrons (N) i.e. $\eta \propto \frac{\partial^2 E}{\partial N^2}$), and quantum mechanical theory for formulating all those global chemical descriptors are quantitatively shown in Eqs. (1−7) [38], [39], [40], [41];

$$IP = -E_{HOMO} \quad (1)$$

$$EA = -E_{LUMO} \quad (2)$$

$$\chi = \frac{(I+EA)}{2} \quad (3)$$

$$\eta = \frac{(-E_{HOMO} + E_{LUMO})}{2} = \frac{Band\ gap\ (\Delta E_{gap})}{2} \quad (4)$$

$$\sigma = \frac{1}{\eta} \quad (5)$$

$$\mu = -\frac{(I+EA)}{2} = -\chi \quad (6)$$

$$\omega = \frac{\mu^2}{2\eta} \quad (7)$$

Being the DFT very promising model for furnishing detailed theoretical/computational insights into the above mentioned global quantum−chemical reactivity parameters, this DFT based theoretical study presents herein a detailed explanation about the HOMO−LUMO interactions and their energy gap (ΔE_{gap}) for each of these two vanadium aquo complex ions: $[V(H_2O)_6]^{2+}$ and $[V(H_2O)_6]^{3+}$ separately on the basis of which their global quantum−chemical reactivity descriptors: *IP*, *EA*, η, σ, μ, ω, and χ are determined to elucidate their relative chemical reactivity or stability kinetically.

3.2.1 HOMO−LUMO analysis and Energy gaps (ΔE_{gap}) for $[V(H_2O)_6]^{2+}$ and $[V(H_2O)_6]^{3+}$ complex ions

As explained in section 3.2, the HOMO and LUMO interactions and their energy gap are very significant quantum mechanical descriptors that can be directly used for deriving the values of wide−ranged global chemical reactivity parameters. The DFT derived surface plots of the HOMO and LUMO for $[V(H_2O)_6]^{2+}$ and $[V(H_2O)_6]^{3+}$ complex ions are shown in Figure 2 and Figure 3, where HOMO energy (E_{HOMO}), LUMO energy (E_{LUMO}), and the HOMO−LUMO energy gaps (ΔE_1 and ΔE_2) are depicted separately. As can be seen in both figures, the HOMO surfaces for the both complex ions are found to be distributed mainly over the central vanadium atoms (coordination centers) while the LUMO surfaces are distributed over almost all the atoms.

.

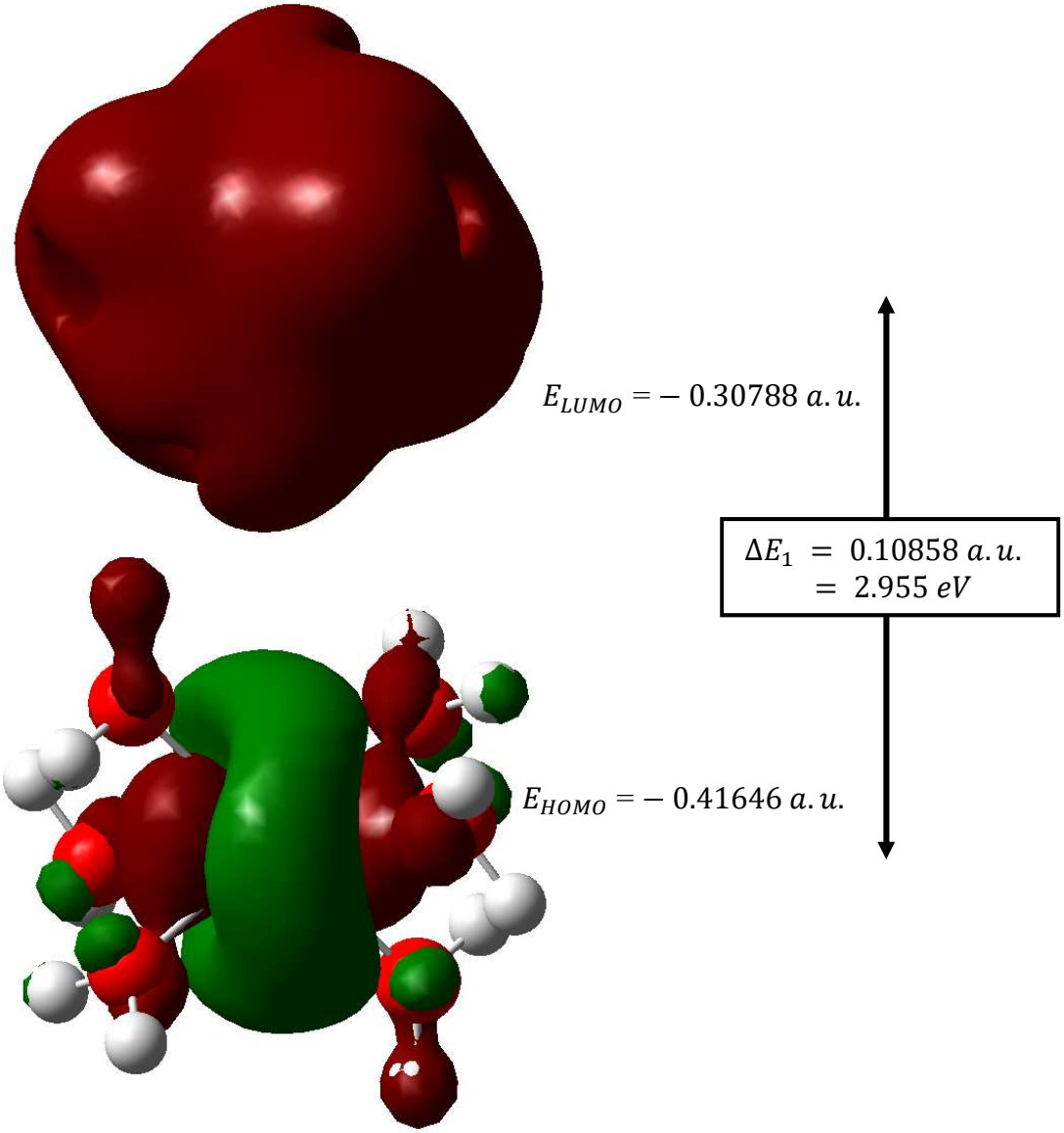

Figure 2. DFT computed surface plots of HOMO and LUMO depicting HOMO−LUMO energy gap ΔE_1 for $[V(H_2O)_6]^{2+}$ complex ion.

These atom centered and localized electron density surfaces indicate that the concerned atomic sites of the complex ions may participate most actively in several types of energy transfer events. Moreover, the HOMO−LUMO energy gaps for both complex ions (depicted in Figure 1 and Figure 2) not only approximate their band gap exists in between valence band and conductance band but also estimate their lowest energy transition frequencies in UV visible spectroscopy. Here, the band gap for the $[V(H_2O)_6]^{3+}$ complex ion ($\Delta E_2 = 2.509\ eV$) (coordination center: V^{3+} has d^2 configuration) is slightly lower than that for the $[V(H_2O)_6]^{2+}$ ($\Delta E_1 = 2.955\ eV$) (coordination center: V^{2+} has d^3 configuration) (Difference = $(\Delta E_1 - \Delta E_2) = 0.446\ eV$), the unpaired electron present in the HOMO of the former ion must undergo faster transition to the LUMO by absorbing specific light ray photons having longer wavelength (λ) than

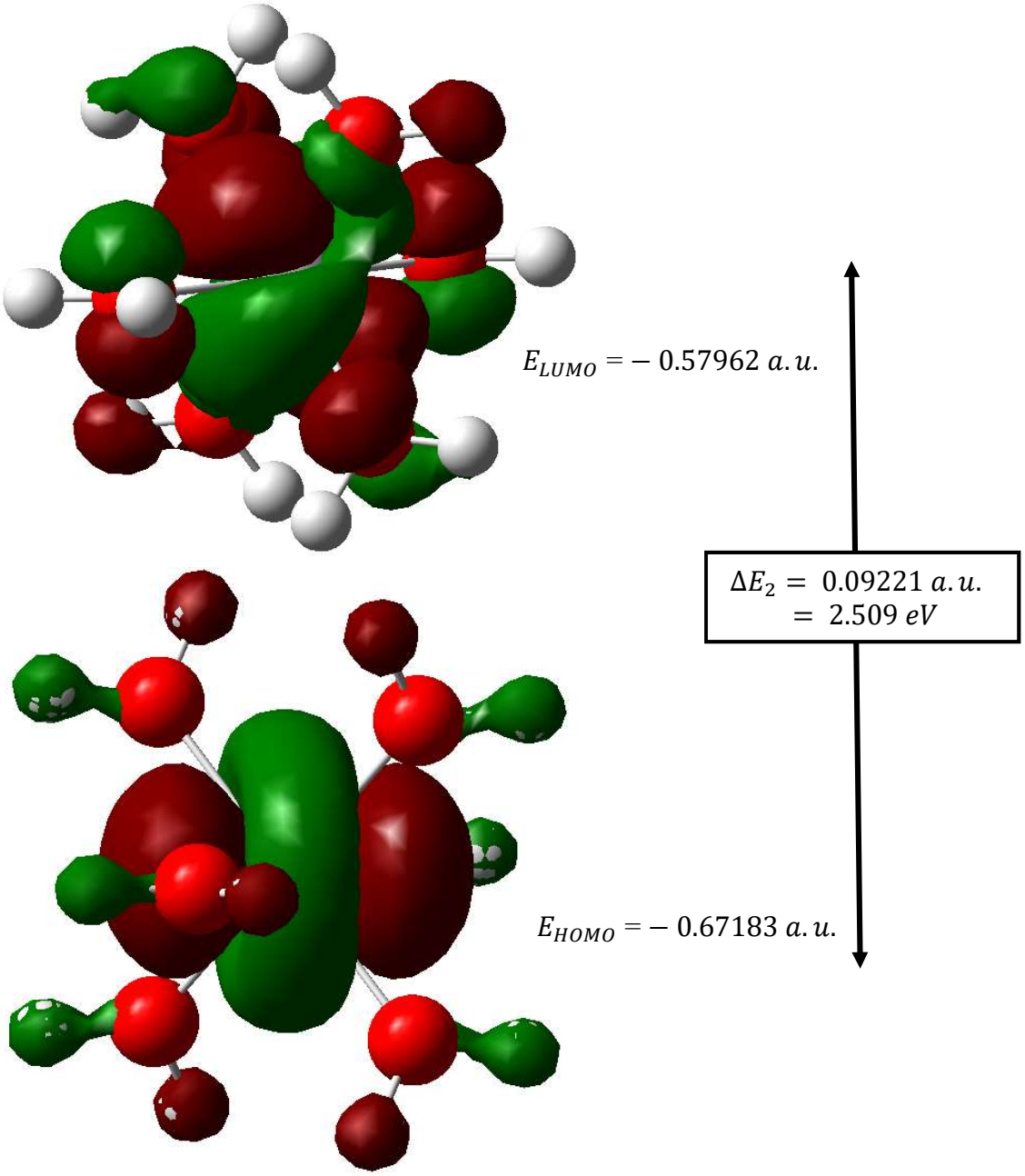

Figure 3. DFT computed surface plots of HOMO and LUMO depicting HOMO-LUMO energy gap ΔE_2 for $[V(H_2O)_6]^{3+}$ complex ion.

that required for the latter ion. Therefore, the wavelengths of the transmitted complementary light for these two complexes must also be different resulting their appearance as green and lilac in color respectively. This qualitative explanation can be clarified with more certainty by utilizing these DFT derived ΔE_1 and ΔE_2 values of the two vanadium aquo complex ions for deriving the exact wavelengths (λ_1 and λ_2) of the respective monochromatic light they should absorb during spectrophotometry (Lambert−Beer law) experiments on the basis of which color of their aqueous solutions can be examined. The concerned mathematical calculations are shown below:

1. For the $[V(H_2O)_6]^{2+}$ complex ion:	**2. For the $[V(H_2O)_6]^{3+}$ complex ion:**
$\Delta E_1 = 2.955\ eV$ (as depicted in Figure 2) $= 4.7344 \times 10^{-19}\ J$; $\therefore \upsilon_1 = 0.7141 \times 10^{15} s^{-1}$ $(\because \Delta E_1 = h\upsilon_1)$ $\therefore \lambda_1 = 420.17\ nm$ $(\because \upsilon_1 = \frac{c}{\lambda_1})$	$\Delta E_2 = 2.509\ eV$ (as depicted in Figure 3) $= 4.0200 \times 10^{-19}\ J$; $\therefore \upsilon_2 = 0.6063 \times 10^{15} s^{-1}$ $(\because \Delta E_2 = h\upsilon_2)$ $\therefore \lambda_2 = 494.81\ nm$ $(\because \upsilon_2 = \frac{c}{\lambda_2})$

Here, values of the $\lambda_1$and λ_2 are approximately found to be $420.17\ nm$ and $494.81\ nm$ respectively for the $[V(H_2O)_6]^{2+}$ and $[V(H_2O)_6]^{3+}$ complex ions. These calculated wavelengths are as consistent as the experimentally observed values for the violet (λ = 380−450 nm), and green (λ = 485−560 nm) colored light of the electromagnetic spectrum, implying that the former complex ion must appear as lilac and the latter as green in color in their ultrapure aqueous solutions.

Similarly, the relatively smaller band gap ΔE_2 of the $[V(H_2O)_6]^{3+}$ complex ion further infers that this ion is more reactive but less stable kinetically than the $[V(H_2O)_6]^{2+}$ i.e. the electrons/ charges of the former ion can migrate from the HOMO to the LUMO more faster than in the latter which eventually enhances the energy transfer events or initiates the molecular chemical reactions (HOMO electrons are very often considered as the most reactive).

3.2.2 Ionization Potential (*IP*), Electron Affinity (*EA*), and Electronegativity (χ) for $[V(H_2O)_6]^{2+}$ and $[V(H_2O)_6]^{3+}$ complex ions

Ionization potential (*IP*) of any molecule is an endothermic energy that simply measures an amount of energy required to remove most loosely bound electron from an isolated molecular species in its ground state [1], [37]. It is used not only to measure the binding force of the electron held by the positively charged nucleus but also to determine the strength of the chemical bonds. Additionally, its absolute value acts as an indicator for the reactivity of the molecules based on the fact that molecules with low *IP* values tend to be oxidized (reducing agents) easily (have high reactivity, less stability and chemical inertness), and can form their cations very likely and vice versa. In contrast to this, an electron affinity (*EA*) of the molecule is an exothermic energy that measures the amount of energy released while adding an extra electron from outside to an isolated molecule in its ground state [1], [38]. The absolute value of it is usually used to identify the nature of the molecular species while monitoring their charge−transfer reactions: molecules having more or less positive *EA* values behave respectively as electron acceptor or donor species. Similarly, the third parameter electronegativity (χ) measures a relative tendency of the bonded atoms or group of atoms in a molecule or molecules themselves to attract shared electron pair towards itself [1]. It is used to detect the polar part/s of the molecule: higher the electronegativity value, the more an atom or a substituent group attracts electrons towards itself creating the oppositely charged terminals. As a whole, all these three parameters are respectively related to the DFT derived energy of the HOMO and LUMO as formulated above in Eq. (1−3). All the calculated values (eV) of them for the $[V(H_2O)_6]^{2+}$ and $[V(H_2O)_6]^{3+}$ complex ions are presented in Table 3. The relatively lower IP value for the $[V(H_2O)_6]^{2+}$ ion (IP = $11.332\ eV$) than that for the $[V(H_2O)_6]^{3+}$ (IP = $18.445\ eV$) signifies that former ion undergoes faster oxidation (i.e. the $[V(H_2O)_6]^{2+}$ ion behaves as a powerful reducing agent: $V^{2+}_{(aq.)} + 2e^- \rightarrow V_{(s)}$; $E^{\circ}_{red} = +1.18V$ and becomes very unstable in the aerated aqueous solution: $^1/_2O_{2(g)} + 2H^+_{(aq.)} + 2e^- \rightleftharpoons H_2O_{(l)}$; $E^{\circ}_{re} = +1.23V$ (reduction half), and $^1/_2O_{2(g)} + 2H^+_{(aq.)} + 2[V(H_2O)_6]^{2+}{}_{(aq.)} \rightarrow 2[V(H_2O)_6]^{3+}{}_{(aq.)} + H_2O_{(l)}$;

$E^{\circ}_{oxi} = -0.26V$ (oxidation half)) than the latter (the $[V(H_2O)_6]^{3+}$ ion behaves as a relatively less powerful reducing agent: $V^{3+}{}_{(aq.)} + 3e^{-} \rightarrow V_{(s)}$; $E^{\circ}_{red} = +0.85V$) whereas a relatively higher EA value for the $[V(H_2O)_6]^{3+}$ ion ($EA = 15.772\ eV$) than that for the $[V(H_2O)_6]^{2+}$ ($EA = 8.377\ eV$) indicates that the former ion has more intensity to accept electrons (electron acceptor) than the latter, clarifying their behavior as an electron acceptor and donor respectively during the electron/charge transfer reactions between themselves: $[V(H_2O)_6]^{2+} + [V(H_2O)_6]^{3+} \rightleftharpoons [V(H_2O)_6]^{3+} + [V(H_2O)_6]^{2+}$ as concluded earlier from the results of Mulliken population analysis method (subsection 3.1.1).

3.2.3 Chemical Hardness (η) and Softness (σ) for $[V(H_2O)_6]^{2+}$ and $[V(H_2O)_6]^{3+}$ ions

According to HSAB principle, the term "hard" has a close connection to those chemical species which are small and weakly polarizable whereas "soft" applies to those which are large and strongly polarizable [35], [36], [37]. In the case of metal−ligand chemistry, the hard metals (hard Lewis acids) are those which have high positive charges, small atomic radii, and have closed shells or half−filled configurations whereas the hard ligands (hard Lewis bases) are those which possess highly electronegative donor atoms such as F, O, and N, small radii, and less polarizable character. As a rule, the hard metals always prefer to coordinate with the hard ligands, and their mutual bonding interactions are mostly electrostatic in nature. Therefore, the hard metals−ligands complex compounds are known for their exceptionally high stability. Accordingly, the corresponding electronic parameters of these two terms: chemical hardness (η) and chemical softness (σ) are those quantum chemical descriptors that can be used to measure the chemical reactivity or stability of the molecular specimens kinetically [40], [41]. As explained in section 3.2, a η has been quantitatively expressed within the DFT computational scheme as a second order derivative of the total energy E of a chemical system with respect to changes in the number of electrons N. On the same basis, a mathematically derived expression for the quantitative estimation of the η is formulated in Eq. (4), where the η shows a direct relation to the HOMO−LUMO interactions and their energy gap (ΔE_{gap}). As given in Eq. (5), an inverse of the η gives chemical softness (σ) which usually measures how intensely the atom or group of atoms acquire electrons. As a rule, lower the value of ΔE_{gap}, lower (higher) will be the value of η (σ), which means more reactive the molecular specimens are. Alternatively, a hard (soft) molecular specimen always has a large (small) ΔE_{gap}, and hence becomes less reactive (more reactive). For the $[V(H_2O)_6]^{2+}$ and $[V(H_2O)_6]^{3+}$ complex ions, the calculated values of η, and σ are listed in Table 3. Even though both of these complex ions involve hard acids (central V^{2+} and V^{3+} ions) and hard bases (H_2O* ligands, * indicates a donor atom), and therefore are thermodynamically stable complexes, their degree of relative hardness and softness can be measured quantitatively by comparing their DFT derived η, and σ values respectively. As can be seen in Table 3, the $[V(H_2O)_6]^{3+}$ ion has a slightly lower (higher) value of the $\eta = 1.336\ eV$ ($\sigma = 0.748\ eV$) than that for the $[V(H_2O)_6]^{2+}$ ion $\eta = 1.477eV$ ($\sigma = 0.677eV$), implying that former ion must be little bit more reactive (or less stable) kinetically, and more strongly polarizable than the latter, and hence can be called as relatively soft molecule.

Table 3. DFT computed quantum chemical descriptors for $[V(H_2O)_6]^{2+}$ and $[V(H_2O)_6]^{3+}$ ions.

Parameters (eV)	Complex ions	
	$[V(H_2O)_6]^{2+}$	$[V(H_2O)_6]^{3+}$
E_{HOMO}	−11.332	−18.445
E_{LUMO}	−8.377	−15.772
ΔE_{gap}	2.955	2.673
IP	11.332	18.445
EA	8.377	15.772
χ	9.854	17.108
η	1.477	1.336
σ	0.677	0.748
μ	−9.854	−17.108
ω	32.871	109.537

3.2.4 Electronic chemical potential (μ) and Electrophilicity index (ω) for $[V(H_2O)_6]^{2+}$ and $[V(H_2O)_6]^{3+}$ complex ions

According to IUPAC definition, the chemical potential (μ) is that electronic parameter which measures the escaping tendency of electrons from one molecular specimen to another during their chemical combination in the ground state conditions [43]. This physical phenomenon occurs on the basis of electronegativity equalization principle: whenever two molecules, X and Y, with $\mu_X > \mu_Y$, approach each other for a polar chemical reaction, the electron density flux from the molecule 'X' transfers towards the molecule 'Y', and attains the equilibrated electronic chemical potential μ_{XY} in the interacting system. In other words, the molecules 'X' and 'Y' behave as electron−donor (nucleophile) and electron−-acceptor (electrophile) respectively, and their difference in the chemical potential $\Delta\mu$ always measures the degree of global electron density transfer (GEDT) [43]. Mathematically, the chemical potential (μ) is a negative of the absolute electronegativity (χ) as formulated in Eq. (6) [41], [42], [43]. As a rule, more negative the μ is, more difficult (easier) is to lose (gain) an electron. Similarly, Parr *et al.* [44] proposed the definition of electrophilicity index (ω) as a measure of energy lowering associated with a maximum amount of electron flow between donor and acceptor species. It estimates the tendency of accepting an extra electron density by the electron−loving chemical species (electrophiles). It is very often used in electrophile−nucleophile chemistry to understand electrophilicity of the majority of the chemical reactions [45]. Mathematically, it is given by the equation formulated in Eq. (7) [41], [42], [43]. As a whole, those chemical compounds which have higher values of μ^2, and ω but lower value of η always behave as the most effective electrophiles. The calculated values of them for the complex ions $[V(H_2O)_6]^{2+}$ and $[V(H_2O)_6]^{3+}$ are given in Table 3. The extremely higher values of μ^2, and ω but relatively lower value of η for the $[V(H_2O)_6]^{3+}$ complex ion ($\mu_1^2 = 292.683\,eV$, $\omega = 109.537\,eV$, $\eta = 1.336\,eV$) than that for the $[V(H_2O)_6]^{2+}$ ($\mu_2^2 = 97.101\,eV$, $\omega = 32.871\,eV$, $\eta = 1.477\,eV$) indicates that former ion has a high degree of electrophilicity or strong electrophilic character (difficult to lose electron) than the latter. The $\Delta\mu\,(\mu_2 - \mu_1)$ value for them is calculated as $7.254\,eV$, indicating that the degree of GEDT between them is comparatively high. It eventually ascertains here a possibility of occurring fast electron transfer reaction between themselves: $[V(H_2O)_6]^{2+} + [V(H_2O)_6]^{3+} \rightleftharpoons [V(H_2O)_6]^{3+} + [V(H_2O)_6]^{2+}$ as interpreted earlier by the Mulliken population analysis and quantum mechanically derived electron affinity (*EA*) values.

IV. Conclusion

Although it is already established from the experimental and theoretical studies that most of the 3*d* transition metals can form very stable homoleptic type metal−aquo complexes $[M(H_2O)_6]^{z+}$ with coordination number equal to 6, the comprehensive research works on electronic charge distributions in them and their relative chemical reactivity or stability through quantum mechanical molecular orbitals approach are seldom reported. More specifically, the extensive computational/theoretical investigations of the Mulliken atomic charge distribution and the global quantum−chemical reactivity descriptors for the vanadium aquo complex ions in oxidation states +II, +III, +IV, and +V are indispensable research topic of current interest due to their predominant availability and crucial roles in catalytic, environmental, industrial, biological, and medicinal aspects of chemistry, and in "all−vanadium" redox flow battery (VRFB) technology. In this contribution, only two vanadium aquo complex ions in the oxidation states +II, and +III, viz., $[V(H_2O)_6]^{2+}$ (lilac), and $[V(H_2O)_6]^{3+}$ (green) were selected on the basis of their typical chemical characteristics such as relatively more chemical instability, fast disproportionation type chemical reactions, oxidation−reduction tendencies, ligand exchange reactions etc., and attempted their Mulliken atomic charges distributions, molecular orbital energy levels, and eigenvalues of the HOMO and LUMO orbitals quantum mechanically (DFT: B3LYP/6−31G (*d*, *p*) methodology) followed by quantitative estimation of the quantum−chemical reactivity parameters: HOMO−LUMO interactions and their energy gap (ΔE_{gap}), ionization potential (*IP*), electron affinity (*EA*), chemical hardness (η), chemical softness (σ), electronic chemical potential (μ), electrophilicity index (ω), and electronegativity (χ).

The theoretically predicted Mulliken charge unit per O atom in $[V(H_2O)_6]^{2+}$ was − 0.66 *a.u.*, 1.37 times, and in $[V(H_2O)_6]^{3+}$ was − 0.67 *a.u.*, 1.92 times, more in electron density than in their centrally located V atoms depicted qualitatively that their coordination centers often act as the most "active−sites" (electron deficient) for initializing redox type chemical reactions. Similarly, the relatively larger value of the HOMO−LUMO band gap for the $[V(H_2O)_6]^{2+}$ complex ion ($\Delta E_{gap} = 2.955\,eV$) than that for the $[V(H_2O)_6]^{3+}$ ($\Delta E_{gap} = 2.673\,eV$) signified that the former ion is less reactive but more stable kinetically than the latter. Moreover,

the theoretically determined wavelengths $\lambda_1 = 420.17\,nm$ (violet colored light) and $\lambda_2 = 494.81\,nm$ (green colored light) of the visible light to be absorbed respectively by these two complex ions confirmed their real practical colors: the former ion always appears as lilac and the latter as green in their aqueous solutions. Most importantly, the theoretically derived values of the global quantum− chemical reactivity parameters ascertained that the $[V(H_2O)_6]^{2+}$ ion relatively: (1) undergoes faster oxidation ($IP = 11.332\,eV$), (2) has a stronger electron donating tendency ($EA = 8.377\,eV$), (3) has a lower polarizability, but higher kinetic stability ($\eta = 1.477eV,\ \sigma = 0.677eV$), (4) has a weaker electrophilic character or less electrophilicity ($\omega = 32.871\,eV$), and (5) loses an electron more easily ($\mu = -9.854\,eV$) than the $[V(H_2O)_6]^{3+}$ ion ($IP = 18.445\,eV,\ EA = 15.772\,eV,\ \eta = 1.336\,eV, \sigma = 0.748\,eV,\ \omega = 109.537\,eV,$ and $\mu = -17.108\,eV$).

Even though above explained DFT derived Mulliken atomic charges distribution, molecular orbital energy levels, HOMO and LUMO interactions and their band gaps (ΔE_{gap}), and the values of the global quantum−chemical reactivity parameters for $[V(H_2O)_6]^{2+}$ and $[V(H_2O)_6]^{3+}$ complex ions could be as reliable as those obtained from high−level computational methods, this research work was only limited to computationally cheap yet decent hybrid density functional B3LYP with 6−31G (*d*, *p*) basis set due to the shortage of enough computational resources. One may use more advanced theoretical models with systematically convergent basis sets recommended for the 3*d* metals such as relativistic and nonrelativistic type that range in quality from triple−ζ to quintuple−ζ [46] to strengthen the results reported here.

REFERENCES

[1] R. D. Madan, "*Modern Inorganic Chemistry*", S. Chand & Company Ltd., **1997**.

[2] J. Krakowiak, D. Lundberg, I. Persson, "A Coordination Chemistry Study of Hydrated and Solvated Cationic Vanadium Ions in Oxidation States +III, +IV, and +V in Solution and Solid State", *Inorganic Chemistry*, Vol. **51**, pp. **9598-9609**, **2012**.

[3] I. Persson, "Hydrated metal ions in aqueous solution: How regular are their structures?", *Pure and Applied Chemistry*, Vol. **82**, Issue **10**, pp. **1901-1917, 2010**.

[4] T. Yamamura, A. B. Marahatta, S. Yoshida, N. Tanno, Inventors; 2016, Tohoku University (Japan), WIPO (PCT) Patent WO2016158295A1.

[5] T. Yamamura, A. B. Marahatta, S. Yoshida, N. Tanno, Inventors; 2016, Tohoku University (Japan), Japan Patent JP2016/057602.

[6] J. B. Foresman, Æ Frisch, "*Exploring Chemistry with Electronic Structure Methods*", Gaussian, Inc., **2015**.

[7] P. Hohenberg, W. Kohn, "Inhomogeneous Electron Gas", *Physical Review B*, Vol. **136**, No. **3B**, pp. **864-871, 1964**.

[8] W. Kohn, L. Sham, "Self-Consistent Equations Including Exchange and Correlation Effects", *Physical Review Journal*", Vol. **140**, No. **4A**, pp. **A1133-A1138**, **1965**.

[9] A. B. Marahatta, "A DFT Analysis for the Electronic Structure, Mulliken Charges Distribution and Frontier Molecular Orbitals of Monolayer Graphene Sheet", *International Journal of Progressive Sciences and Technologies,* Vol. **16,** Issue **1**, pp. **51-65**, **2019**.

[10] A. B. Marahatta, "Effect of n-Type Dopant Nitrogen in the Structure and Atomic Charges Distribution of Monolayer Graphene Sheet: A DFT Analysis", *International Journal of Progressive Sciences and Technologies,* Vol. **16,** Issue **2**, pp. **01-13**, **2019**.

[11] A. B. Marahatta, "DFT Study on Ground State Electronic Structures of Simple to Complex Molecular Specimens", *International Journal of Progressive Sciences and Technologies*, Vol. **19,** Issue **1**, pp. **100-112**, **2020**.

[12] A. B. Marahatta, H. Kono, "Comparative Theoretical Study on the Electronic Structures of the Isolated Molecular Gyroscopes with Polar and Nonpolar Phenylene Rotator", *International Journal of Progressive Sciences and Technologies,* Vol. **20,** Issue **1**, pp. **109-122**, **2020**.

[13] A. B. Marahatta, "Computational Study on Electronic Structure, Atomic Charges Distribution and Frontier Molecular Orbitals of Butadiene: General Features for Diels-Alder Reaction", *International Journal of Progressive Sciences and Technologies,* Vol. **19,** Issue **2**, pp. **48-64**, **2020**.

[14] A. J. Cohen, P. M. Sánchez, W. Yang, "Insights into current limitations of density functional theory", *Science*, Vol. **321**, Issue **5890**, pp.**792-794**, **2008**.

[15] A. B. Marahatta, "Towards Understanding the Stabilities of Hydrated Vanadium (V) Complex Ions and the Pathway of V_2O_5 Precipitation in Catholyte Solution of Vanadium Redox Flow Battery", *International Journal of Progressive Sciences and Technologies,* Vol. **20**, Issue **2**, pp. **348-364**, **2020**.

[16] M. Bühl, H. Kabrede, "Geometries of Transition-Metal

Complexes from Density-Functional Theory", *Journal of Chemical Theory and Computations*, Vol. **2**, Issue **5**, pp. **1282-1290**, **2005**.

[17] B. I. Kruft, "Density Functional Theory for the Investigation of Transition Metal Complexes: Structure, Binding, and Spectroscopy of Metal-Siderophores and the Catalase-Peroxidase Enzyme", A dissertation submitted as part of the requirements for the degree of Doctor of Philosophy (Ph. D.), The City University of New York, USA, **2015**.

[18] C. J. Cramer, D. G. Truhlar, "Density functional theory for transition metals and transition metal chemistry", *Physical Chemistry Chemical Physics*, Vol. **11**, Issue **46**, pp. **10757-10816**, **2009**.

[19] A. C. Tsipis, "DFT flavor of coordination chemistry", *Coordination Chemistry Reviews*, Vol. **272**, pp. **1-29**, **2014**.

[20] B. Kallies, R. Meier, "Electronic Structure of 3d $[M(H_2O)_6]^{3+}$ Ions from Sc^{III} to Fe^{III}: A Quantum Mechanical Study Based on DFT Computations and Natural Bond Orbital Analyses", *Inorganic Chemistry*, Vol. **40**, Issue **13**, pp. **3101-3122**, **2001**.

[21] R.C. Maurya, B.A. Malik, J.M. Mir, P.K. Vishwakarma, "Oxidovanadium(IV) complexes involving dehydroacetic acid and β-diketones of bioinorganic and medicinal relevance: Their synthesis, characterization, thermal behavior and DFT aspects", *Journal of Molecular Structure*, Vol. **1083**, pp. **343-356**, **2015**.

[22] B. Mukherjee, B. Patra, S. Mahapatra, P. Banerjee, A. Tiwari, M. Chatterjee, "Vanadium-an element of atypical biological significance", *Toxicology Letters*, Vol. **150**, Issue **2**, pp. **135-143**, **2004**.

[23] A. F. Rowley, "The blood cells of the sea squirt, *Ciona intestinalis*: Morphology, differential counts, and *in vitro* phagocytic activity", *Journal of Invertebrate Pathology*, Vol. **37**, Issue **1**, pp. **91-100**, **1981**.

[24] J. C. Pessoa, S. Etcheverry, D. Gambino, "Vanadium compounds in medicine", *Coordination Chemistry Reviews*, Vol. **301**, pp. **24-48**, **2015**.

[25] A. Bishayee, A. Waghray, M. A. Patel, M. Chatterjee, "Vanadium in the Detection, Prevention and Treatment of Cancer: The in Vivo Evidence", *Cancer Letter*, Vol. **294**, Issue **1**, pp. **1-12**, **2010**.

[26] MedicineNet, VANADIUM, *https://www.medicinenet.com/vanadium/supplements-vitamins.htm*

[27] R. S. Mulliken, "Electronic Population Analysis on LCAO–MO Molecular Wave Functions. I", *Journal of Chemical Physics*, Vol. **23**, pp. **1833-1840**, **1955**.

[28] A. Bendjeddou, T. Abbaz, S. Maache, R. Rehamnia, A. K. Gouasmia, D. Villemin, "Quantum chemical descriptors of some paminophenyl tetrathiafulvalenes through density functional theory (DFT)", *RASAYAN Journal of Chemistry*, Vol. **9**, No. **1**, pp **18-26**, **2016**.

[29] W. Locke, "*Introduction to Molecular Orbital Theory*", ICSTM Chemistry Department, **1996**.

[30] **Æ. Frisch, H. P. Hratchian, R. D. Dennington II, T. A. Keith, J. Millam, "***Gauss view 05 Reference,* Gaussian, Inc. **2009**.

[31] Gaussian 09 manual. *http://gaussian.com/geom/?tabid=1#GeomkeywordReadOptimi zeoption*

[32] Æ Frisch, "*Gaussian 09W Reference",* Gaussian, Inc., **2009**.

[33] M. D. Segall, R. Shah, C. J. Pickard, M. C. Payne, "Population analysis of plane-wave electronic structure calculations of bulk materials", *Physical Review B*, Vol. **54**, No. **23, 16317- 16320**, **1996**.

[34] K. Fukui, "Role of Frontier Orbitals in Chemical Reactions", *Science*, Vol. **218**, No. **4574** pp. **747-754**, **1982**.

[35] *W. L. Jolly, "Modern Inorganic Chemistry", McGraw-Hill Book Company, New York, **1984**.*

[36] E. C. Koch, "Acid-Base Interactions in Energetic Materials: "I. The Hard and Soft Acids and Bases (HSAB) Principle-Insights to Reactivity and Sensitivity of Energetic Materials", *Propellants, Explosives, Pyrotechnics*, Vol. **30**, Issue **1**, pp. **5-16**, **2005**.

[37] R. G. Parr, R. G. Pearson, "Absolute hardness: companion parameter to absolute electronegativity", *Journal of American Chemical Society*, Vol. **105**, Issue **26**, pp. **7512–7516**, **1983**.

[38] M. S. A. Abdel-Mottaleb, S. N. Ali, "A New Approach for Studying Bond Rupture/Closure of a Spiro Benzopyran Photochromic Material: Reactivity Descriptors Derived from Frontier Orbitals and DFT Computed Electrostatic Potential Energy Surface Maps", *International Journal of Photoenergy*, Article ID **6765805**, pp. **1-9**, **2016**.

[39] S. Kumar, A. Syed, S. Andotra, R. Kaur, Vikas, S. K. Pandey, "Investigation of synthesized new vanadium(III) complexes of ditolyldithiophosphate ligands by spectroscopic, cyclic voltammetric, DFT, antimicrobial and cytotoxic studies", *Journal of Molecular Structure*, Vol. **1154**, Issue **2018**, pp. **165-178**, **2017**.

[40] M. Saranya, S. Ayyappan, R. Nithya, R. K. Sangeetha, A. Gokila, "Molecular structure, NBO and HOMO-

LUMO analysis of quercetin on single layer graphene by density functional theory", *Digest Journal of Nanomaterials and Biostructures*, Vol. **13**, No. **1**, pp. **97-105**, **2018**.

[41] T. Abbaz, A. Bendjeddou, D. Villemin, "Molecular orbital studies (hardness, chemical potential, electro negativity and electrophilicity) of TTFs conjugated between 1, 3-dithiole", *International Journal of Advanced Research in Science, Engineering and Technology*, Vol. **5**, Issue **2** , pp. **5150-5161**, **2018**.

[42] A. D. McNaught, A. Wilkinson, "IUPAC. Compendium of Chemical Terminology, 2nd ed. (the "Gold Book")", Blackwell Scientific Publications, Oxford, 1997.

[43] L. R. Domingo, M. Ríos-Gutiérrez, P. Pérez, "Applications of the Conceptual Density Functional Theory Indices to Organic Chemistry Reactivity", *Molecules*, Vol. **21**, Issue **748**, pp. **1-22**, **2016**.

[44] R. G. Parr, L. V. Szentpály, S. Liu, "Electrophilicity Index", *Journal of American Chemical Society*, Vol. **121**, Issue **9**, pp. **1922-1924**, **1999**.

[45] P. K. Chattaraj, U. Sarkar, D. R. Roy, "Update 1 of: Electrophilicity Index", *Chemical Review*, Vol. **107**, Issue **9**, pp. **46−74**, **2007**.

[46] N. B. Balabanov, K. A. Peterson, "Systematically convergent basis sets for transition metals. I. All-electron correlation consistent basis sets for the 3d elements Sc–Zn", *Journal of Chemical Physics*, Vol. **123**, pp **064107(1-15)**, **2005**.